


Fast volumetric imaging with line-scan confocal microscopy by electrically tunable lens at resonant frequency: supplement

KHUONG DUY MAC,¹  MUHAMMAD MOHSIN QURESHI,² MYEONGSU NA,³ SUNGHOE CHANG,^{3,4} TAE JOONG EOM,^{5,6} HYUNSOO SHAWN JE,^{7,8} YOUNG RO KIM,^{9,10} HYUK-SANG KWON,^{1,13} AND EUIHEON CHUNG^{1,11,12,14}

¹Department of Biomedical Science and Engineering, Gwangju Institute of Science and Technology, Gwangju 61005, Republic of Korea

²Division of Biophysics and Bioimaging, Princess Margaret Cancer Centre, Toronto, ON, Canada

³Department of Physiology and Biomedical Sciences, Seoul National University College of Medicine, 103 Daehak-ro, Jongno-gu, 03080 Seoul, Republic of Korea

⁴Neuroscience Research Institute, Seoul National University College of Medicine, 103 Daehak-ro, Jongno-gu, 03080 Seoul, Republic of Korea

⁵Department of Cogno-Mechatronics Engineering, Pusan National University, Busan, 46241, Republic of Korea

⁶Engineering Research Center (ERC) for Color-modulated Extra-sensory Perception Technology, Pusan National University, Busan, 46241, Republic of Korea

⁷Signature Program in Neuroscience and Behavioural Disorders, Duke-National University of Singapore (NUS) Medical School, 8 College Road 169857, Singapore

⁸Advanced Bioimaging Center, Academia, Ngee Ann Kongsi Discovery Tower Level 10, 20 College Road, 169855, Singapore

⁹Athinoula A. Martinos Center for Biomedical Imaging, Massachusetts General Hospital, Charlestown, Massachusetts 02129, USA

¹⁰Department of Radiology, Harvard Medical School, Boston, Massachusetts 02115, USA

¹¹AI Graduate School, Gwangju Institute of Science and Technology, Gwangju 61005, Republic of Korea

¹²Research Center for Photon Science Technology, Gwangju Institute of Science and Technology, Gwangju 61005, Republic of Korea

¹³hyuksang@gist.ac.kr

¹⁴ogong50@gist.ac.kr

This supplement published with Optica Publishing Group on 17 May 2022 by The Authors under the terms of the [Creative Commons Attribution 4.0 License](https://creativecommons.org/licenses/by/4.0/) in the format provided by the authors and unedited. Further distribution of this work must maintain attribution to the author(s) and the published article's title, journal citation, and DOI.

Supplement DOI: <https://doi.org/10.6084/m9.figshare.19683915>

Parent Article DOI: <https://doi.org/10.1364/OE.450745>

Fast volumetric imaging with line-scan confocal microscopy by electrically tunable lens at resonant frequency: supplemental document

KHUONG DUY MAC,¹MUHAMMAD MOHSIN QURESHI,²MYEONGSU NA,³SUNGHOE CHANG,^{3,4}TAE JOONG EOM,^{5,6}HYUNSOO SHAWN JE,^{7,8}YOUNG RO KIM,^{9,10}HYUK-SANG KWON,^{1,13}AND EUIHEON CHUNG^{1,11,12,14}

¹*Department of Biomedical Science and Engineering, Gwangju Institute of Science and Technology, Gwangju 61005, South Korea*

²*Division of Biophysics and Bioimaging, Princess Margaret Cancer Centre, Toronto, ON, Canada*

³*Department of Physiology and Biomedical Sciences, Seoul National University College of Medicine, 103 Daehak-ro, Jongno-gu, 03080 Seoul, South Korea*

⁴*Neuroscience Research Institute, Seoul National University College of Medicine, 103 Daehak-ro, Jongno-gu, 03080 Seoul, South Korea*

⁵*Department of Cogno-Mechatronics Engineering, Pusan National University, Busan, 46241, South Korea*

⁶*Engineering Research Center (ERC) for Color-modulated Extra-sensory Perception Technology, Pusan National University, Busan, 46241, South Korea*

⁷*Signature Program in Neuroscience and Behavioural Disorders, Duke-National University of Singapore (NUS) Medical School, 8 College Road, Singapore 169857*

⁸*Advanced Bioimaging Center, Academia, Ngee Ann Kongsi Discovery Tower Level 10, 20 College Road, Singapore 169855*

⁹*Athinoula A. Martinos Center for Biomedical Imaging, Massachusetts General Hospital, Charlestown, Massachusetts 02129, USA*

¹⁰*Department of Radiology, Harvard Medical School, Boston, Massachusetts 02115, USA*

¹¹*AI Graduate School, Gwangju Institute of Science and Technology, Gwangju 61005, South Korea*

¹²*Research Center for Photon Science Technology, Gwangju Institute of Science and Technology, Gwangju 61005, South Korea*

¹³hyuksang@gist.ac.kr

¹⁴ogong50@gist.ac.kr

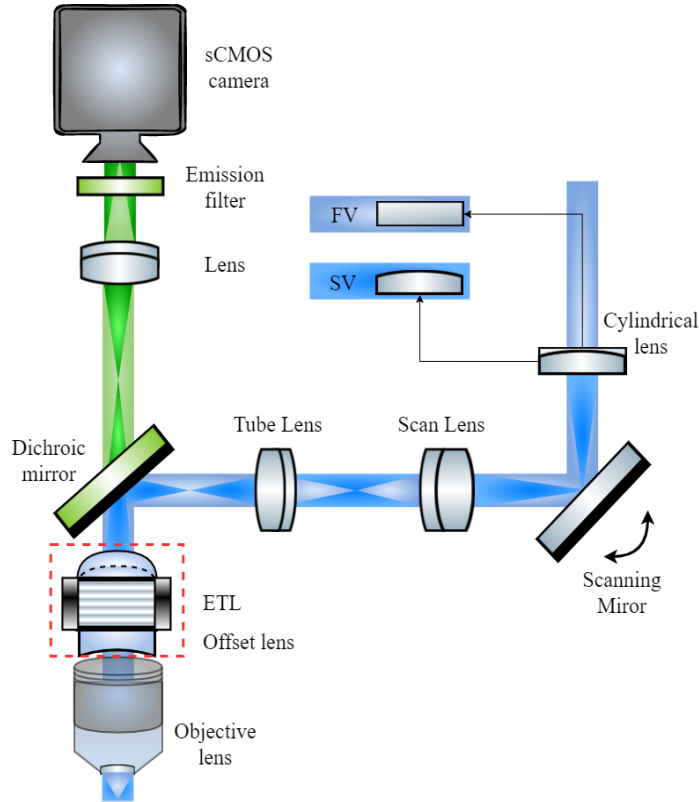


Figure S1. Schematics of the ETL-based LSCM where the ETL is positioned above the objective lens with the offset lens (concave lens), a conventional ETL configuration

In our first configuration, the ETL was placed right before the objective lens, in which the excitation light entering the back focal plane of the objective lens would vary, resulting in the changes of resolution with respect to the changing ETL focal length. The laser beam size is magnified 3 times by a 4-f system ($f = 50$ mm and $f = 150$ mm, respectively) before it propagates the cylindrical lens ($f_{\text{cyl}} = 50$ mm) to generate the line pattern at the image plane, parallel to the x-axis. Here we use the one-direction scanning mirror (re-modified from Thorlabs GVS002) right after the cylindrical lens to perform the sweeping of laser in the range of 4-degree angles, parallels to y-axis. The scanning of the mirror combines the line patterns from the cylindrical lens to produce full images. Then the elliptical beam propagates the Scan lens ($f_{\text{scan}} = 60$ mm) and Tube lens ($f_{\text{TL}} = 250$ mm) to conjugated with the back focal plane of the objective. A dichroic mirror (Semrock, FF552-Di02-25x36) and the ETL (Optotune, EL-10-30-C-VIS-LD) system are placed in between the Tube lens and Objective lens (Olympus, 20X 0.5 NA, water immersion, UMPLFLN20XW) to enable the axial scanning and guide the detection path follows along the scan path. We place a plano-concave lens ($f = -50$ mm) to prevent the aberration that normally occurs in the imaging system. The combination of ETL and offset lens (box with red dotted line) was replaced with ETL with a tube lens in the asLSCM system. The fluorescent signal after excitation from the sample propagates the dichroic mirror. An achromatic doublet lens ($f = 150$ mm) is placed in between the dichroic mirror and detector, the position of the lens is conjugated with the back focal plane of the objective lens and the detector surface. A sCMOS camera is used to capture the full image which is swept by the scanner mirror. To compare the profiles of the PSF of the asLSCM and the conventional system with ETL-offset lens, the tube lens was removed while the ETL combined with an offset lens

was placed right beneath the objective lens. This was the initial first generation of the imaging system and the detail of the diagram was described in the Figure S1.

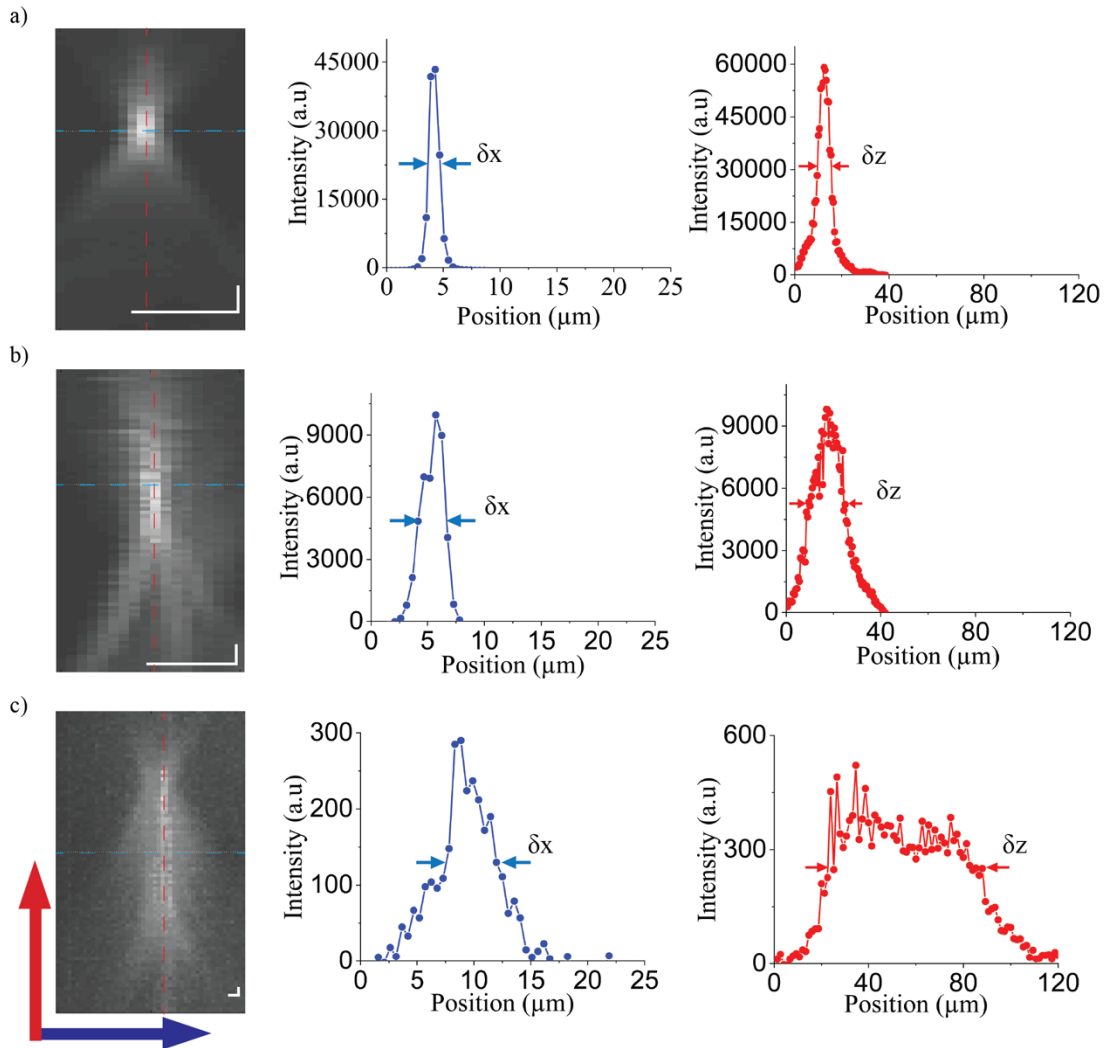


Figure S2. Comparison of PSF profiles of the system in Figure S1. Lateral (blue) and axial (red) PSF of ETL-based LSCM produced without ETL related 4-f system using 0.5 μm fluorescent beads where a) ETL and offset lens were removed, b) ETL and offset lens were attached but not activated (stationary mode), and c) ETL was activated with the sinusoidal current function between 0mA to 60mA at around ~350 Hz. Scale bar: 5 μm .

We activated the ETL in two different categories to compare the resolution in each stage: without ETL, ETL off (stationary stage), and ETL dynamic stage. At the first stage, the obtained lateral full-width-half-maximum (FWHM) achieved was $\delta x = 0.8 \pm 0.01 \mu\text{m}$ ($n=3$) with the axial resolution FWHM was $\delta z = 6.3 \pm 0.1 \mu\text{m}$ ($n=3$) (Fig. S2a). We then attached the ETL with an offset lens in the system. Therefore, the combination with an objective lens may degrade the system fidelity, resulting in the lateral and axial resolution were $\delta x = 1.5 \pm 0.1 \mu\text{m}$ ($n=3$) and $\delta z = 18.7 \pm 0.8 \mu\text{m}$ ($n=3$), respectively (Figure S2b). The lateral FWHM, $\delta x = 5.2 \pm 0.1 \mu\text{m}$ ($n=3$) with the activated ETL for the dynamic stage while in the axial direction, the FWHM of value was extended; $\delta z = 65 \pm 2.2 \mu\text{m}$ ($n=3$) from the axial scanning by the ETL (Figure S2c).

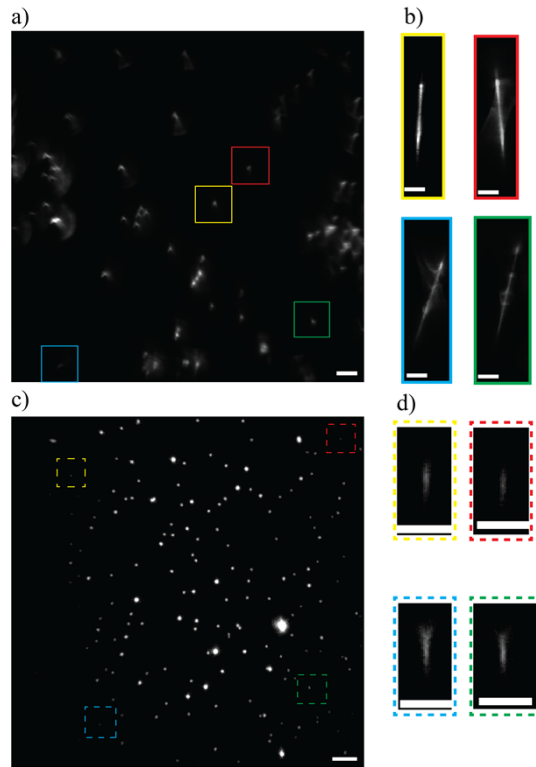


Figure S3. Evaluation of the PSF distortion with the activated ETL using fluorescent beads of $0.5\ \mu\text{m}$ for volumetric imaging and standard line-scan confocal microscopy: a) asLSCM and c) standard LSCM. The field of view analyses were performed displaying the PSF profiles in the axial direction, b) asLSCM, and d) standard LSCM. Scale bar: $25\ \mu\text{m}$.

We further analyzed the aberration properties of our ETL-based asLSCM system by evaluating the shapes of the axial penetration of point spread function (PSF; Fig. S3a). At the center region of the FOV, PSF geometry did not change much axially and remained almost straight, while further away from the center, greater tilt of the PSF (Fig. S3b) was observed. Additionally, the PSF from the standard line-scan confocal microscopy (Fig. S3c and S3d) exhibited a marginal aberration.

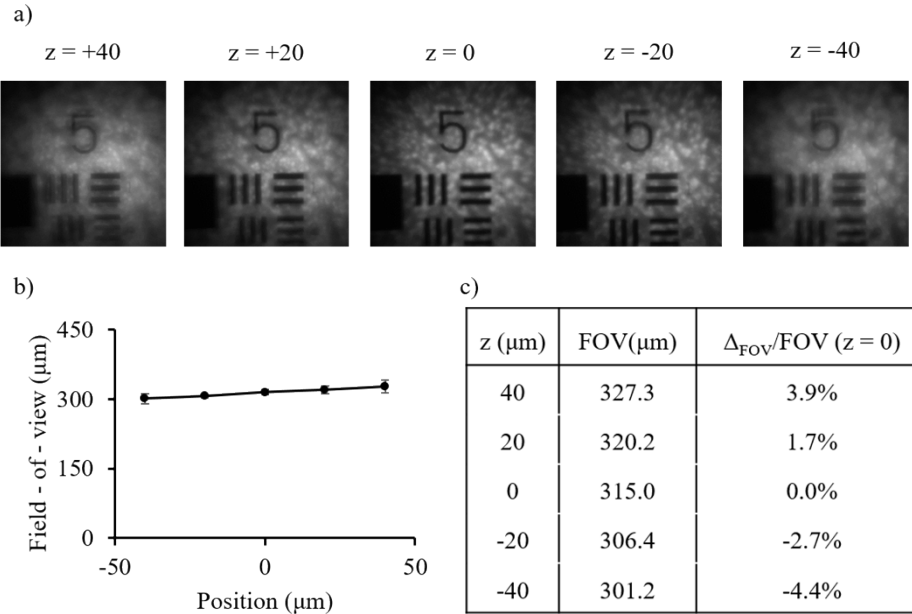


Figure S4. Evaluation of the field of view (FOV) at different axial layers under resonant ETL mode (-40, -20, 0, +20, +40 μm), a) the images of fluorescent USAF target at different layers, b) the relationship between the one axis in FOV and layer position (z), c) relative change of other z position $\Delta_{\text{FOV}}/\text{FOV}$ at position z = 0 μm.

However, with the ETL activated in the resonant mode, the FOV of the system did not change much. For the demonstration, an experiment was performed to acquire images of the USAF target at different axial positions with the system running in the resonant mode (Fig. S4a) where the z = 0 position was defined as the focused position, identified under the stationary mode with the ETL driven at 140 mA. The total FOV of all images was measured, in which at lower the positions in axial direction, smaller FOV's were observed (Fig. S4b). However, as calculated, the percent change in FOV was less than $\pm 5\%$ (Fig. S4c), indicating that there were not significant layer-dependent magnifications in the current volumetric image.